Proceedings of ISFOG 2025
5TH INTERNATIONAL SYMPOSIUM ON
FRONTIERS IN OFFSHORE GEOTECHNICS
Nantes, France | June 9-13 2025
© 2025 the Authors
ISBN 978-2-85782-758-0

Centrifuge modelling to investigate the response of caisson anchor under uplift monotonic loading

A. Sahare*
Tokyo City University, Tokyo, Japan

K. Sano, Y. Kawahara, K. Itoh
Tokyo City University, Tokyo, Japan

**sahare@tcu.ac.jp (corresponding author)*

ABSTRACT: This study investigates the uplift response of caisson anchors embedded in dry sand under varying inclined monotonic loading conditions using a geotechnical centrifuge. Three loading scenarios were examined: purely vertical, inclined at 60°, and inclined at 16°. Load-displacement behavior and failure envelopes were analyzed, along with 3D evolution of axial force, bending moment, and displacement data. Results show that while uplift capacities under vertical and 60° loading were comparable, the 16° inclined case produced significantly larger displacements and internal forces. The inclined loading cases introduced notable bending moments due to horizontal load components, with maximum values increasing as the inclination angle decreased. Spatial variations along the anchor shaft revealed non-uniform stress development, especially under low-angle diagonal loading. High-speed video and schematic observations confirmed that inclined loading causes tilting, mobilizing passive earth pressure and enhancing soil-anchor interaction. These effects significantly elevate both bending and axial tensile forces. The findings highlight the necessity of accounting for combined axial and lateral load paths in design, especially for offshore mooring applications.

Keywords: Floating wind turbine; anchoring; uplifting mechanism, geotechnical centrifuge modelling, monotonic loading

1 INTRODUCTION

Several parts of the world are experiencing rising temperatures, an increase in severe floods, typhoons, and drought due to climate change. This has motivated several states to explore options in offshore renewable energy to substantially reduce reliance on fossil fuel industries. Additionally, recent geopolitical events have resulted in significant inflation, which could be mitigated if energy production were localized using offshore wind turbines. The current global offshore wind capacity stands at 75.3 GW as per the Global Wind Report (2024), with China and Europe contributing more than 90% of this capacity. To satisfy the Paris Agreement, the global offshore target needs to increase at an annual rate of 80 GW until 2030 (Cerfontaine et al., 2023). However, new offshore installations in 2023 only contributed an additional 10.8 GW, which is far below the required level.

One major reason is the very limited installation of floating-type wind turbine systems worldwide. The availability of shallow waters around Europe and Asia has allowed large-scale deployment of wind turbines on fixed-type foundations such as monopiles or suction bucket foundations, and significant knowledge has been established for such systems under environmental and seismic loading (Espanol-Espinel et al., 2024; Liu & Kaynia, 2021; Takahashi et al., 2022; Ueda et al., 2020). In contrast, less than 0.2% of the current offshore renewable energy capacity comes from floating wind turbines. Clearly, the installation of floating-type wind turbines will play a critical role in achieving the net-zero target set by various countries. This is particularly relevant for Japan, which has significant potential for floating offshore wind.

Anchoring plays a crucial role in the overall stability of floating wind turbines throughout their operational lifetime. However, since floating wind turbines are still in the early stages of development, fewer studies have investigated the anchoring response to environmental loading. Lu et al. (2020) examined the drained response of rigid piles in dense sand under inclined tensile loads. Their findings highlighted the coupled development of axial tension and bending moment due to load inclination. In addition, some research has also been performed on plate-type anchors (Roy et al., 2022), pore pressure generation in surrounding sand may result in loss of embedment (Chow et al., 2020). The inability to predict embedment loss during keying and monotonic-cyclic

loading makes plate-type anchors vulnerable to subsequent loading cycles. On the other hand, caisson-type anchors are better suited for floating applications due to their high load-bearing capacity and efficient installations. However, the load magnitude applied to the anchor depends on the mooring system (i.e., catenary, taut mooring, or tension-leg mooring). Based on mooring line configurations, floating platforms can be classified into Tensioned Leg Platforms (TLPs), spars, semi-submersibles, or barges. Unfortunately, there is limited research on understanding the mobilized shear stresses, axial stresses, and bending moments along the soil-anchor interface when a vertical caisson anchor undergoes monotonic uplift under different mooring scenarios (i.e., purely vertical uplift versus inclined uplift). Inclined loading introduces both horizontal and vertical load components, necessitating differentiation from the purely vertical loading condition.

2 GEOTECHNICAL CENTRIFUGE MODELLING

By subjecting a small-scale caisson anchor model to an increased gravitational field, realistic stress-strain conditions can be imposed. Data obtained from geotechnical centrifuge modeling can validate numerical tools and provide further insights into measured phenomena (Sahare et al., 2020, 2024a). This study employed the newly developed geotechnical centrifuge facility (TCU Mark III) at Tokyo City University, Japan. The beam-type centrifuge has an effective diameter of 2.8 m and can carry a maximum payload of 10 g-ton under a maximum operational centrifugal acceleration of 100g. Figure 1 shows a picture of the centrifuge device. Further details regarding this centrifuge facility can be found in Sahare et al. (2025).

Figure 1 – Newly installed Mark III centrifuge facility at Tokyo City University, Japan.

2.1 Centrifuge experimental program

Figure 2 presents a typical model layout for the centrifuge testing. A rigid box container with an internal width of 300 mm (15 m in prototype) and a height of 180 mm (9 m in prototype) was used. The caisson anchor model, with an outer diameter of 40 mm (2 m in prototype) and a thickness of 1 mm, was fabricated using aluminum. The anchor length was 120 mm (6 m in prototype). Toyoura sand (e_{min} = 0.608, e_{max} = 0.951, G_s = 2.659), a uniform fine sand with a fines content of less than 0.1%, was used at a relative density of 60%. Toyoura sand has been extensively utilized in previous centrifuge experiments in Japan (e.g., Sahare et al., 2022). Further details regarding Toyoura sand's response under monotonic and cyclic loading can be found in Umar et al. (2021) and Yang & Sze (2011).

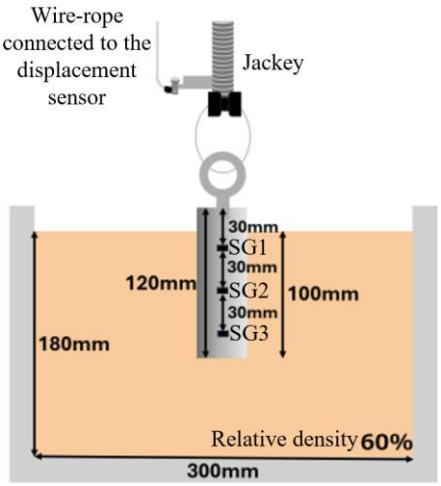

Figure 2 – Cross section of the developed centrifuge model.

Three centrifuge experiments were conducted on the caisson anchor model under different monotonic loading scenarios. Case-1 involved purely vertical uplift loading simulating a typical TLP floating wind turbine. Case-2 involved monotonic inclined uplift loading at a 60° angle with the horizontal. On the other hand, Case-3 involved an anchor loaded monotonically at an inclination of 16 degrees. Although fully saturated soil conditions are ideal for studying undrained-partially drained loading responses, for simplicity, dry sand conditions resembling drained conditions were used in this study. It is worth noting that resembling a caisson anchor in this manner reduces its capacity against uplift loading, providing insight into its mechanics under a worst-case scenario.

Toyoura sand was air-pluviated in layers, adjusting the free-fall height to maintain consistent density

throughout the model. The caisson anchor was instrumented with strain gauges at three locations at 30 mm intervals (1.5 m in prototype) as shown in Fig. 2 to measure axial force and bending moment profiles during monotonic uplift loading. The caisson anchor was installed mechanically at 1g conditions using a mounted actuator device (Figure 3). Support beams ensured verticality during installation. The anchor was placed sufficiently far from the model container's side boundaries to avoid boundary effects (Ullah et al., 2016).

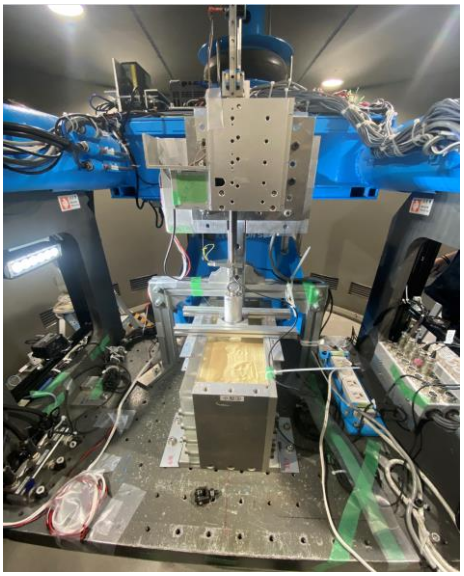

Figure 3 – Picture of the centrifuge setup to apply uplift monotonic loading to the pile anchor (prior to anchor installation).

During spin-up operation to 50g centrifugal acceleration, the anchor was allowed to settle freely with the surrounding soil. The anchor model remained in place for 5-10 minutes (in model scale) to achieve stable instrumentation readings before uplift loading. The monotonic uplift load was applied using a wire rope assembly connected to a load cell mounted inside the actuator as shown in Fig. 3. The vertical uplift displacement was measured using a separate wire rope assembly in tension.

In Case-1, the anchor was installed directly below the actuator for purely vertical uplift loading. In Case-2 and 3, the anchor was installed vertically, but the load was applied at a 60° and 16° inclination at the top, ensuring realistic force transmission.

2.2 Results and discussion

Three distinct loading conditions were assessed to understand the impact of loading inclination on the anchor's displacement response, with each case showing both the uplift vertical load-displacement curves and corresponding failure envelopes in Figures 4, 5, and 6.

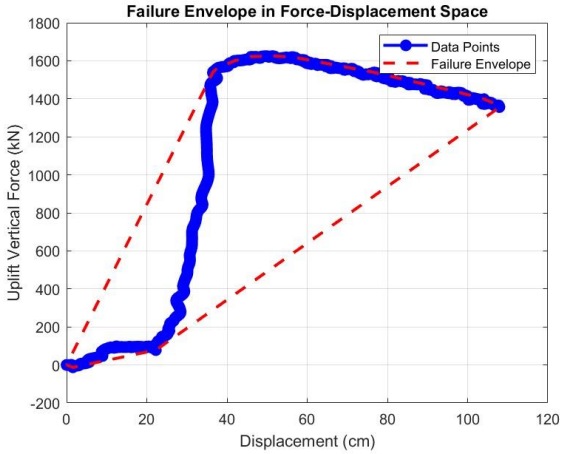

Figure 4 – Case_1_Purely vertical uplift loading.

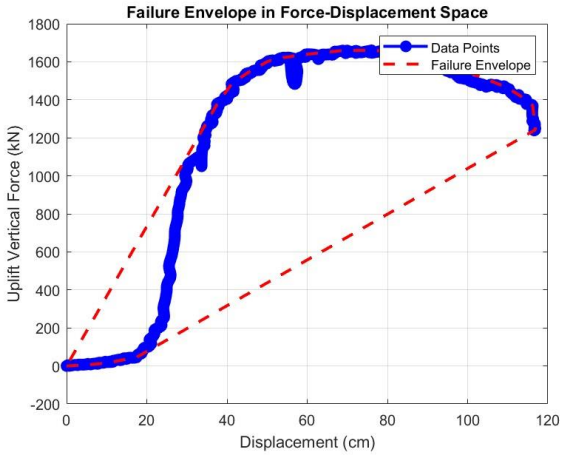

Figure 5 – Case_2_Inclined uplift loading at 60° inclination.

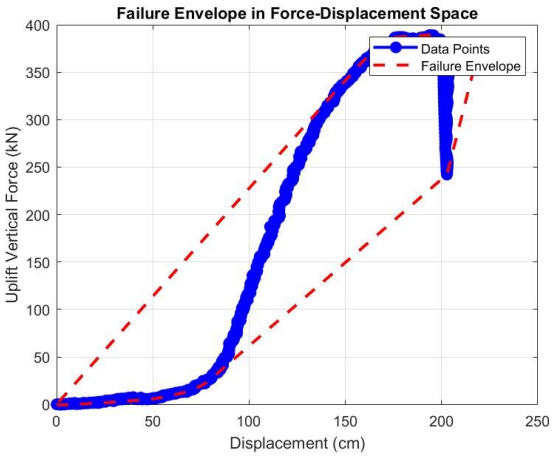

Figure 6 – Case_3_Inclined uplift loading at 16° inclination.

Figure 4 shows an initial increase in vertical uplift load with displacement, indicating an elastic-plastic

soil response, before reaching a peak uplift resistance. Beyond this peak, the vertical load remains relatively constant for a displacement of approximately 20 cm, thereafter slightly decreasing, suggesting ultimate uplift capacity has been reached. The anchor experiences further displacement with no additional increase in resistance, indicative of plastic soil behavior and anchor failure.

In Figure 5, the anchor's response under loading inclined at 60 degrees from the horizontal is presented. The vertical uplift capacity is comparable to the purely vertical scenario. The initial load-displacement behavior demonstrates gradual mobilization of uplift force, reaching peak resistance at a displacement magnitude relatively larger compared to the purely vertical case. This resulted in the failure envelope acquiring a larger area. Post-peak, a notable decline in resistance indicates significant horizontal and vertical force interaction, resulting in plastic deformation and anchor displacement.

Figure 6 illustrates the caisson anchor under monotonic loading inclined at 16 degrees from the horizontal. The uplift resistance gradually increases with displacement, achieving peak capacity at a displacement significantly larger than observed in Cases 1 and 2. Post-peak, the resistance suddenly decreases at a nearly constant magnitude of displacement, indicating major horizontal components influencing soil yielding and anchor displacement.

Overall, the experimental results demonstrate that inclination affects the anchor's force-displacement behavior due to altered soil-anchor interaction. The integrated failure envelopes in Figures 4 to 6 clearly illustrate the coupling effects between horizontal and vertical forces, emphasizing the importance of these interactions for accurate design and analysis of caisson anchors.

The comparison of bending moment versus displacement for Case 1 and Case 2 reveals key differences in structural response due to loading inclination as shown in Figure 7. In Case 1 (purely vertical), the bending moment remains minimal across all displacement levels, indicating that the anchor is primarily subjected to axial tension with negligible lateral components. This confirms minimal flexural demand and highlights a dominantly vertical load path. In contrast, Case 2 (inclined at 60 degrees) exhibits a significantly higher bending moment, with a peak exceeding 100 kN-m. This pronounced flexural response is due to the introduction of substantial lateral force components through inclined loading, which induces bending in the caisson shaft. The bending moment rises quickly during initial loading, stabilizes near the peak uplift force, and then gradually decreases during post-peak displacement. This behavior underlines the rotational and shear effects induced by inclined loading, which must be considered in anchor design under non-vertical mooring systems.

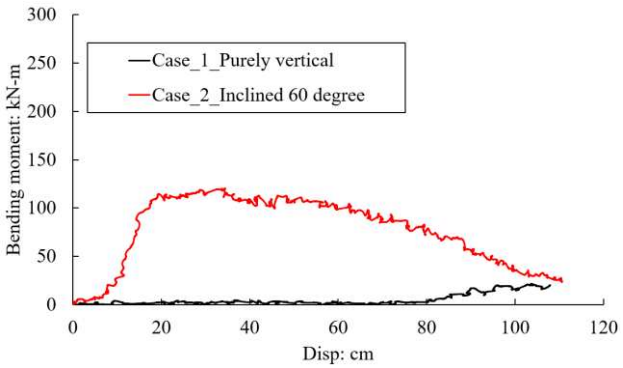

Figure 7 – Mobilization of bending moment (at SG3) and displacement in Case 1 and Case 2.

The 3D load path for Case 1, presented in the figure 8, illustrates the evolution of axial force, bending moment, and displacement throughout the loading process. The path starts at zero displacement with a small axial force and no bending moment. As the displacement increases, the axial force grows steadily while the bending moment oscillates within a narrow range around zero, confirming that the load remains predominantly axial. This reinforces the observation that Case 1 is governed by minimal flexural interaction and behaves nearly as a pure tension anchor. The trajectory ultimately stabilizes at higher displacement levels as the anchor reaches failure, depicted by the red endpoint on the curve.

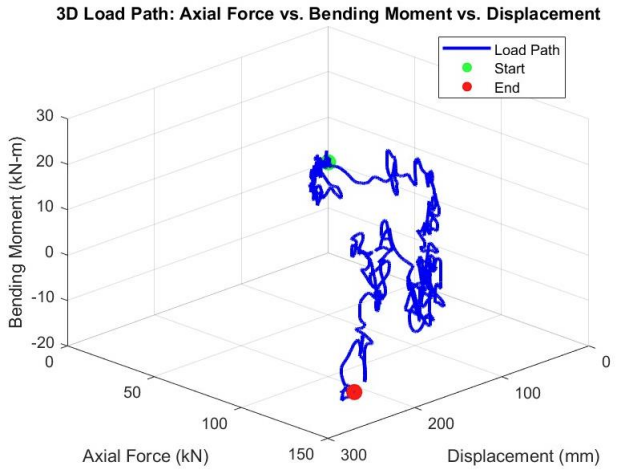

Figure 8 – Evolution of Bending moment, axial force and displacement in Case 1

The 3D load path for Case 2 reveals a much more complex trajectory than Case 1, highlighting the increased interaction between axial and lateral forces due to inclined loading as shown in Figure 9. Initially,

both axial force and bending moment increase steadily with displacement. As the loading continues, the bending moment reaches considerably higher values, consistent with prior observations from the bending moment–displacement graph. The trajectory exhibits fluctuations and loops, indicating shifting dominant load components and significant structural interaction. The final segment of the path shows a drop in axial force while the bending moment continues to vary, illustrating a redistribution of stresses as the anchor approaches failure. The end point, marked in red, captures the system state at large displacements and reduced load-carrying capacity, emphasizing the nonlinear and coupled nature of the response under inclined uplift.

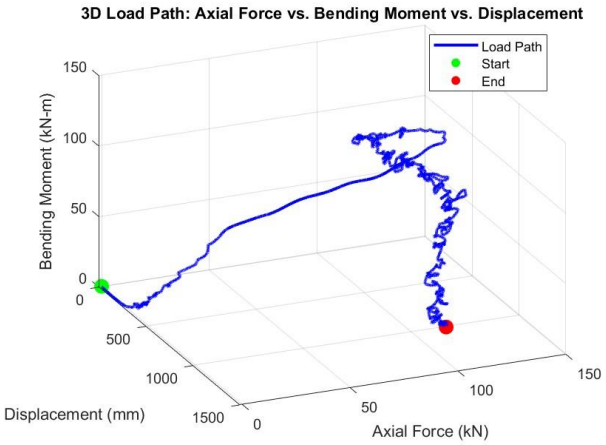

Figure 9 – Evolution of Bending moment, axial force and displacement in Case 2

The 3D load path comparison between two spatial locations along the anchor shaft (strain gauge positions SG1 and SG2) provides deeper insights into internal force development in Case 3 as presented in Figure 10. It is observed that both the load paths exhibit an initial rise in axial force and displacement, accompanied by an increase in bending moment. However, the magnitude and shape of the paths vary significantly between locations. SG1, positioned higher along the shaft, reaches peak bending moments earlier, while SG2 captures larger displacements and delayed curvature. These differences emphasize the non-uniform distribution of internal stresses along the anchor. Notably, both the axial force and bending moment magnitudes in Case 3 are significantly larger than those in Cases 1 and 2. This substantial increase is primarily attributed to the pronounced horizontal load component in the 16-degree inclined loading condition, which amplifies flexural effects and overall structural demand on the anchor.

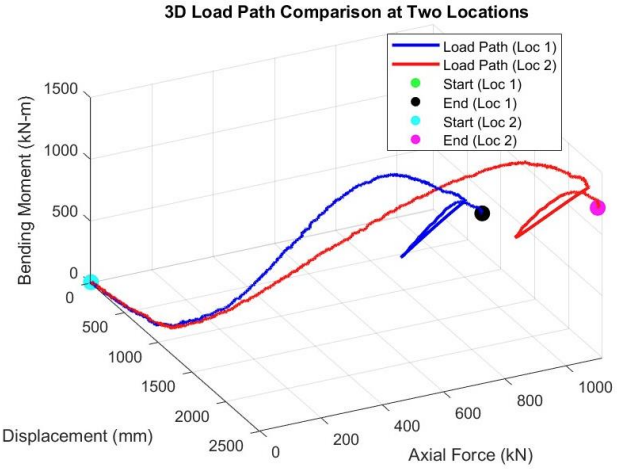

Figure 10 – Evolution of Bending moment, axial force and displacement at locations SG1 and SG2 in Case 3

2.3 Loading mechanism and soil-structure interaction

Figure 11 shows the behavior of the pile during pull-out, captured from HDV camera footage positioned at the side of the soil tank. Under vertical pull-out, the pile moves strictly upward, maintaining alignment. However, in diagonal pull-out scenarios, horizontal displacement is also introduced, causing the pile to tilt in the direction of the applied load. In diagonal pull-out, the pile tilts, generating significant passive resistance. The smaller the angle of diagonal pull-out (i.e., closer to horizontal), the greater the horizontal force developed at the top of the pile. This increase leads to a corresponding rise in the bending moment experienced by the pile. Similarly, axial tensile forces also increase with decreasing pull-out angle.

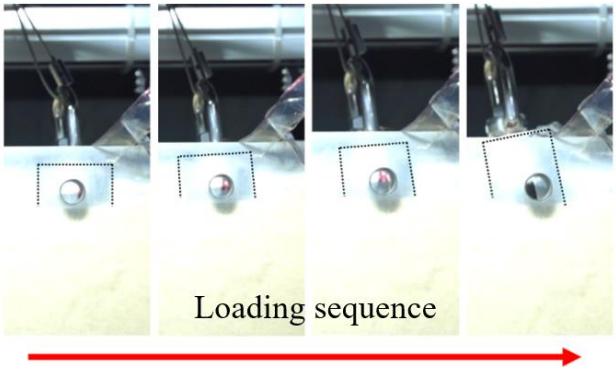

(a)

(b)

Figure 11 – (a) Loading sequency (b) state of the pile after the experiment in Case-2

Notably, a linear relationship was observed between the peak axial tensile force and maximum bending moment in the pile. This suggests that as the bending moment increases due to greater lateral displacement and passive earth pressure, so does the axial load. Thus, inclined loading causes more substantial mobilization of both axial and bending responses in the anchor, which must be carefully accounted for in geotechnical anchor design involving non-vertical loads.

3 CONCLUSIONS

The geotechnical centrifuge experiments conducted under varying loading inclinations revealed critical insights into the uplift behavior and soil-structure interaction mechanisms of caisson anchors in dry sand. The results confirm that loading inclination significantly influences both the magnitude and nature of anchor resistance and internal structural responses.

- Effect of Inclination on Uplift Capacity: While vertical and moderately inclined loading (60°) resulted in similar peak uplift capacities, a shallower inclination (16°) produced the largest displacements and notably different load paths, highlighting the strong impact of horizontal load components.
- Failure Mechanism and Load Transfer: Load-displacement and failure envelope analyses demonstrated that as the angle of inclination decreases, the anchor transitions from primarily axial loading to a combined axial-bending state, with post-peak softening more prominent under inclined loading.
- Bending Moment and Structural Response: Bending moment–displacement results revealed that inclined loading introduces significant flexural demand on the anchor shaft. Case 2 exhibited over tenfold increases in peak bending moment compared to vertical loading, and Case 3 presented even higher magnitudes due to enhanced horizontal forces.
- 3D Load Path Analysis: The 3D load path trajectories highlighted the coupling between axial force, bending moment, and displacement. Case 3, especially at multiple strain gauge locations, showed complex and non-uniform stress development.
- Soil-Structure Interaction Mechanisms: High-definition footage and schematics confirmed that inclined loading induces tilting, passive earth pressure mobilization, and additional frictional resistance along the pile. This leads to a proportional increase in both axial tensile and bending forces as the inclination angle decreases.

Overall, the study demonstrates that diagonal uplift loading results in more complex interaction mechanisms and structural demands. These findings underline the necessity for design approaches that explicitly consider the combined effects of vertical and horizontal loading components, especially for offshore or mooring applications where inclined anchor loading is common.

AUTHOR CONTRIBUTION STATEMENT

Anurag Sahare: Conceptualization, Methodology, Investigation, Funding acquisition, Data curation, Formal Analysis, Supervision, Writing- Original draft. **Kazuya Sano**: Methodology, Investigation. **Yuzuki Kawahara**: Data curation, Investigation. **Kazuya Itoh**: Supervision, Funding acquisition.

REFERENCES

Cerfontaine, B., White, D., Kwa, K., Gourvenec, S., Knappett, J., & Brown, M. (2023). Anchor geotechnics for floating offshore wind: Current technologies and future innovations. *Ocean Engineering, 279*, 114327. https://doi.org/10.1016/j.oceaneng.2023.114327

Chow, S. H., Diambra, A., O'Loughlin, C. D., Gaudin, C., & Randolph, M. F. (2020). Consolidation effects on monotonic and cyclic capacity of plate anchors in sand. *Geotechnique, 70*(8), 720–731. https://doi.org/10.1680/jgeot.19.TI.017

Español-Espinel, C., Haigh, S. K., Madabhushi, G. S. P., Abadie, C. N., Go, J. E., & Morrison, P. R. J.

(2024). Evolution of excess pore water pressures around monopiles subjected to moderate seismic loading. *Soil Dynamics and Earthquake Engineering, 176*, 108316. https://doi.org/10.1016/j.soildyn.2023.108316

Global Wind Energy Council. (2024). *Global Wind Report 2024*. https://gwec.net/global-wind-report-2024/. (accessed 28/11/2024).

Liu, H., & Kaynia, A. (2021). Characteristics of cyclic undrained model SANISAND-MSu and their effects on response of monopiles for offshore wind structures. *Geotechnique, 73*(4), 294–309. https://doi.org/10.1680/jgeot.21.00068

Lu, T., O'Loughlin, C. D., Gaudin, C., & White, D. J. (2020). Drained response of rigid piles in sand under an inclined tensile load. *Géotechnique Letters, 10*(2), 173–179. https://doi.org/10.1680/jgele.19.00028

NEDO. (2024). *NeoWins (offshore wind condition map)*. https://appwdc1.infoc.nedo.go.jp/Nedo_Webgis/. (accessed 28/11/2024).

Roy, A., O'Loughlin, C. D., Chow, S. H., & Randolph, M. F. (2022). Inclined loading of horizontal plate anchors in sand. *Geotechnique, 72*(12), 1051–1067. https://doi.org/10.1680/jgeot.20.P.119

Sahare, A., Choi, G. C., & Ueda, K. (2024a). Role of initial static shear on the cyclic response of saturated backfill retained by a sheet-pile wall: Insights from the strain space multiple mechanism model. *Soil Dynamics and Earthquake Engineering, 179*, 108542. https://doi.org/10.1016/j.soildyn.2024.108542

Sahare, A., Sano, K., Itoh, K., Suemasa, N., Tanaka, T., Torita, M., & Takeoka, R. (2025). Development of a novel cylindrical cam shaking table for geotechnical centrifuge modelling. *International Journal of Physical Modelling in Geotechnics, 25*(2), 66–85. https://doi.org/10.1680/jphmg.24.00032

Sahare, A., Tanaka, Y., & Ueda, K. (2020). Numerical study on the effect of rotation radius of geotechnical centrifuge on the dynamic behavior of liquefiable sloping ground. *Soil Dynamics and Earthquake Engineering, 138*, 106339. https://doi.org/10.1016/j.soildyn.2020.106339

Sahare, A., Ueda, K., & Uzuoka, R. (2022). Influence of the sloping ground conditions and the subsequent shaking events on the pile group response subjected to kinematic interactions for a liquefiable sloping ground. *Soil Dynamics and Earthquake Engineering, 152*, 107036. https://doi.org/10.1016/j.soildyn.2021.107036

Takahashi, A., Omura, N., Kobayashi, T., Kamata, Y., & Inagaki, S. (2022). Centrifuge model tests on large-diameter monopiles in dense sand subjected to two-way lateral cyclic loading in short-term. *Soils and Foundations, 62*(3), 101148. https://doi.org/10.1016/j.sandf.2022.101148

Ueda, K., Uzuoka, R., Iai, S., & Okamura, T. (2020). Centrifuge model tests and effective stress analysis of offshore wind turbine systems with a suction bucket foundation subject to seismic load. *Soils and Foundations, 60*(6), 1546–1569. https://doi.org/10.1016/j.sandf.2020.08.007

Ullah, S. N., Hu, Y., Stanier, S., & White, D. (2016). Lateral boundary effects in centrifuge foundation tests. *International Journal of Physical Modelling in Geotechnics, 17*(3), 144–160. https://doi.org/10.1680/jphmg.15.00034

Umar, M., Chiaro, G., Kiyota, T., & Ullah, N. (2021). Deformation and cyclic resistance of sand in large-strain undrained torsional shear tests with initial static shear stress. *Soils and Foundations, 61*(3), 765–781. https://doi.org/10.1016/j.sandf.2021.02.008

Yang, J., & Sze, H. Y. (2011). Cyclic behavior and resistance of saturated sand under non-symmetrical loading conditions. *Geotechnique, 61*(1), 59–73. https://doi.org/10.1680/geot.9.P.019

Zhou, Z., O'Loughlin, C. D., White, D. J., & Stanier, S. A. (2020). Improvements in plate anchor capacity due to cyclic and maintained loads combined with consolidation. *Geotechnique, 70*, 732–749. https://doi.org/10.1680/jgeot.19.TI.028

INTERNATIONAL SOCIETY FOR
SOIL MECHANICS AND
GEOTECHNICAL ENGINEERING

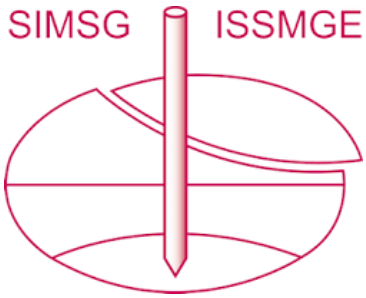

This paper was downloaded from the Online Library of the International Society for Soil Mechanics and Geotechnical Engineering (ISSMGE). The library is available here:

https://www.issmge.org/publications/online-library

This is an open-access database that archives thousands of papers published under the Auspices of the ISSMGE and maintained by the Innovation and Development Committee of ISSMGE.

The paper was published in the proceedings of the 5th International Symposium on Frontiers in Offshore Geotechnics (ISFOG2025) and was edited by Christelle Abadie, Zheng Li, Matthieu Blanc and Luc Thorel. The conference was held from June 9th to June 13th 2025 in Nantes, France.